Hindawi
Shock and Vibration
Volume 2021, Article ID 5510879, 10 pages
https://doi.org/10.1155/2021/5510879

Research Article

Fault Diagnosis of Rolling Bearing Using Improved Wavelet Threshold Denoising and Fast Spectral Correlation Analysis

Shaoning Tian,[1] Dong Zhen,[1] Junchao Guo,[1] Haiyang Li,[2] Hao Zhang,[1] and Fengshou Gu[2]

[1]*Tianjin Key Laboratory of Power Transmission and Safety Technology for New Energy Vehicles, School of Mechanical Engineering, Hebei University of Technology, Tianjin 300401, China*
[2]*Centre for Efficiency and Performance Engineering, University of Huddersfield, Huddersfield HD1 3DH, UK*

Correspondence should be addressed to Dong Zhen; d.zhen@hebut.edu.cn and Haiyang Li; haiyang.li@hud.ac.uk

Received 25 January 2021; Revised 28 March 2021; Accepted 8 April 2021; Published 20 April 2021

Academic Editor: Huaitao Shi

Rolling bearings are important parts of mechanical equipment. However, the early failures of the bearing are usually masked by heavy noise. This brings about difficulties to the extraction of its fault features. Therefore, there is a need to develop a reliable method for early fault detection of the bearing. Considering this issue, a novel fault diagnosis method using the improved wavelet threshold denoising and fast spectral correlation (Fast-SC) is proposed. First, to solve the discontinuity of the hard threshold function and avoid the constant deviation triggered by the soft threshold function, a piecewise continuous threshold function is proposed by using a new threshold selection rule to denoise the original signal. In the new threshold function, the adjuster α is introduced to improve the traditional wavelet denoising algorithm, so as to enhance the signal-to-noise ratio (SNR) of the original signal more effectively. Then, the denoised signal is analysed by Fast-SC to identify the rolling bearing fault features. Finally, simulation analysis and experimental data demonstrate that the proposed approach is effective for rolling bearing fault detection compared with Fast-SC and the combined method based on traditional wavelet threshold and Fast-SC.

1. Introduction

Rolling bearings are widely used in rotating machinery. However, they are also the most susceptible to be damaged in mechanical systems. As one of the most important fault sources of mechanical equipment, any fault of the bearing will seriously affect the performance of the entire machine. If the fault cannot be discovered and diagnosed in time, it will cause serious personal injury and unnecessary economic loss [1–5]. Therefore, monitoring the running condition of the rolling bearing and finding out its early failure in time is of great significance to the safety of its operation. In recent years, more and more approaches have been raised to detect the failures of rolling bearings, including vibration, acoustic emission, sound, temperature, and wear debris analyses [6–10]. Among them, vibration analysis can reflect the dynamic behavior of rolling bearing systems availably and contains abundant fault information, so it has been widely used.

Currently, numerous typical signal processing methods are used for fault diagnosis of rolling bearings. Although these methods have been proven to be effective for rolling bearing defect detection, they still have inherent limitations. For example, Rajiv and Peng [11] proposed a fault diagnosis method for detecting rotor faults by using STFT. Although STFT has the advantages of simple calculation method, easy implementation, and no cross-term interference, it has the defects of high redundancy, limited time-frequency aggregation, and lack of adaptability. Asr et al. [12] put forward a feature extraction method using EMD. The extracted features are input into non-naïve Bayesian classifier to realize rotating mechanism fault diagnosis. However, the end effect and modal aliasing of EMD may cause the IMF to lose its specific physical significance. Li et al. [13] put forward a method for extracting nonstationary vibration feature of gearboxes based on the sparse decomposition. Sparse decomposition has better signal decomposition performance,

but it depends on the design and decomposition algorithm of the atomic library. Li et al. [14] proposed a fault diagnosis method using time-delay feedback monostable stochastic resonance (SR). The SR is an effective tool for extracting transient features, but its detection capability is limited because its system parameters are difficult to determine. Li et al. [15] used SVD to acquire the fault feature of bearings. Although SVD is an effective noise reduction method, its effectiveness cannot be maintained when the measured signal has a low signal-to-noise ratio (SNR).

In recent years, spectral correlation (SC) has played a strong part in the extraction of fault features of rotating machinery. It simultaneously displays the modulations and carriers of a signal in the form of a bispectral map. SC is a prime tool for second-order cyclostationary analysis, so it has received extensive attention in the field of rotating machinery fault diagnosis [16–18]. Liu and Gryllias [19] put forward a semisupervised support vector data description fault detection method using cyclic spectrum analysis and verified the feasibility of the method. Liu et al. [20] used nonlinear spectral correlation to detect fatigue cracks under noisy environments. The results prove that the sensitivity of nonlinear spectral correlation to fatigue cracks is higher than the classical nonlinear coefficient. Although the capabilities of SC in condition monitoring have been confirmed in some research works, in some cases, the expensive computational costs of SC limit its application. Fast spectral correlation (Fast-SC) is a new spectral correlation estimation means proposed by Antoni et al. [21]. This method not only retains the advantage of fast calculation speed of SC but also overcomes the defect of expensive calculation costs. Therefore, Fast-SC has achieved good results in the fault diagnosis of rotating machinery. Li et al. [22] used sparse code shrinkage denoising and Fast-SC to detect rolling bearing faults. The results prove that this method has acquired ideal results in the detection of rolling bearing faults. Tang and Tian [23] proposed a rolling bearings compound fault diagnosis method using singular negentropy difference spectrum and integrated Fast-SC. The results show that this method is very effective for the separation of rolling bearing composite faults. But the fault signals of rolling bearings usually contain strong noise. It is found through research that the presence of noise will seriously interfere with the analysis effect of Fast-SC. Wavelet transform (WT) is widely applied in signal processing. WT is suitable for disposing nonstationary and nonlinear signals because of its characteristics such as low entropy, multiresolution, and flexibility of base selection. Among them, the wavelet hard and soft threshold denoising method proposed by Donoho and Johnstone [24] in 1994 has been widely used due to its small amount of calculation and easy implementation. However, due to the discontinuity of the hard threshold function and the constant deviation caused by the soft threshold method, the traditional threshold function cannot obtain ideal effects in signal denoising. Therefore, selecting the appropriate threshold function is one of the key problems for wavelet threshold denoising algorithm. In this paper, a new improved threshold function is proposed to improve the deficiency of traditional threshold function, and a regulator α is introduced to change the shape of the threshold curve by adjusting the value of α, which makes the threshold processing of wavelet coefficient more flexible.

Considering the above problems, this paper presents a novel time-frequency analysis method combining improved wavelet threshold denoising and Fast-SC for rolling bearing fault diagnosis. First, the improved wavelet threshold denoising algorithm is applied to eliminate the noise component of the original signal and improve the SNR of the original signal. Then Fast-SC analysis is devoted to the denoised signal to enhance the periodic component of the signal and accurately extract the fault characteristic frequency of the bearing. Finally, the reliability of this approach is verified by simulation and experimental analysis. Compared with the Fast-SC and the combined method using traditional wavelet threshold and Fast-SC, the proposed approach can accurately detect bearing faults.

This paper is organized as follows: In Section 2, the detailed implementation process of the proposed approach is provided. Section 3 introduces the basic theory of improved wavelet threshold denoising algorithm. The principle of the Fast-SC is proposed in Section 4. In Section 5, this method is confirmed by simulation analysis. In Section 6, a case of the outer race fault of the motor rolling bearing is used to evaluate this method. Finally, conclusions are given in Section 7.

2. Algorithmic Flow of the Improved Wavelet Threshold Denoising and Fast-SC

Motivated by the advantages of improved wavelet threshold denoising and Fast-SC, this paper proposes a fault diagnosis method using improved wavelet threshold denoising and Fast-SC for rolling bearings. The structural framework of this approach is shown in Figure 1.

3. Improved Wavelet Threshold Denoising

3.1. The Principle of Wavelet Threshold Denoising. In actual engineering, the measured signals are usually mixed with different degrees of noise. Broadly speaking, a signal model with noise can be expressed as

$$s(t) = f(t) + n(t), \tag{1}$$

where $s(t)$ is the original signal, $f(t)$ is the useful signal, and $n(t)$ is random noise.

In general, the useful signal is chiefly distributed in the region of the low frequency, and the high-frequency area is mainly distributed with noise. The purpose of wavelet denoising is to suppress $n(t)$ and reproduce $f(t)$. Therefore, the principle of wavelet threshold denoising is to select a suitable threshold to process the wavelet coefficients; the wavelet coefficients below the threshold are set to 0, while those above the threshold are retained. Finally, the retained wavelet coefficients are used to reconstruct the denoised signal. The algorithm mainly consists of three steps [25]. The specific process is shown in Figure 2.

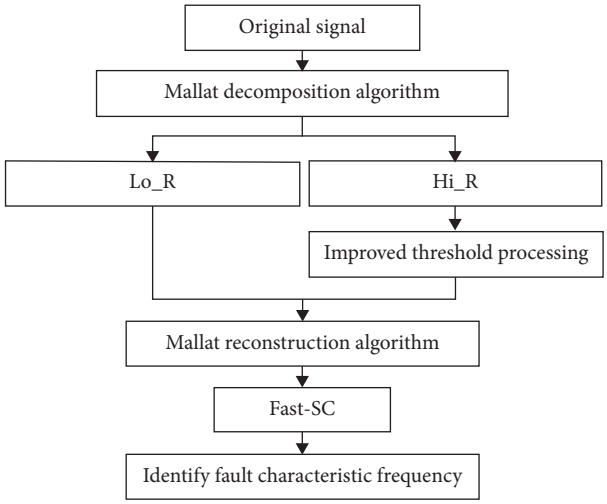

Figure 1: The flowchart of this methodology.

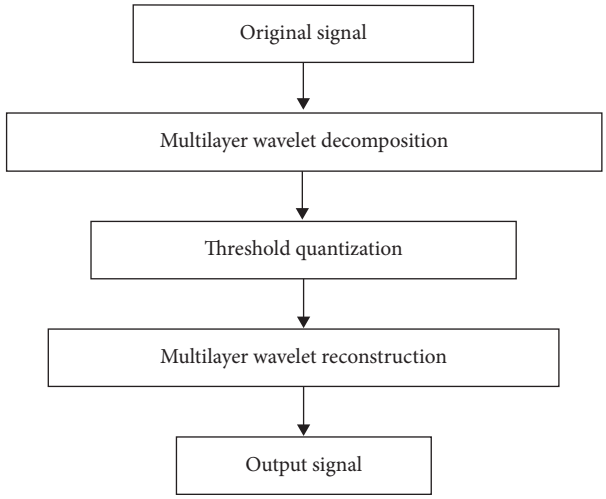

Figure 2: The flowchart of wavelet threshold denoising algorithm.

(1) The discrete wavelet base is used to decompose the signal and analyze the signal features of each layer to obtain approximation coefficients and detail coefficients

(2) The detail coefficients are disposed by using threshold function and applicable threshold

(3) The approximate coefficients and the modified detail coefficients are used to reconstruct the signal

3.2. Wavelet Threshold. Wavelet threshold denoising needs to set a threshold; the ideal threshold can remove the noise component and recover the useful information effectively. At present, the unified threshold proposed by Donoho et al. [23, 24] has been broadly used, as shown in the following equation:

$$\lambda = \sigma\sqrt{2\ln N}, \tag{2}$$

where N is the length of signal and σ is the standard deviation of noise. In engineering applications, the noise standard deviation is generally calculated by the following equation:

$$\sigma = \frac{\text{median}\left(\left|\mathscr{W}_{1,k}\right|\right)}{0.6745}, \tag{3}$$

where $\mathscr{W}_{1,k}$ is the original wavelet coefficient and median$(*)$ is the intermediate value function.

The noise energy will decrease as the decomposition scale increases, so the threshold should also decrease with the increase of the decomposition scale. At the same time, the noise standard deviation of the wavelet coefficients of each layer should be estimated, respectively. The stratification threshold is applied to process the wavelet coefficients of each layer, and the equation is as follows:

$$\begin{cases} \lambda_i = \dfrac{\sigma_i\sqrt{2\ln N_i}}{\ln(i+1)}, \\ \\ \sigma_i = \dfrac{\text{median}\left(\left|\mathscr{W}_{i,k}\right|\right)}{0.6745}, \end{cases} \tag{4}$$

where i is the number of decomposition layers and N_i is the length of the wavelet coefficients of the i-th layer. λ_i will decrease as the number of decomposed layers augments, which can effectively retain the effective signal under high decomposition layers.

3.3. Threshold Processing Function

3.3.1. Traditional Wavelet Threshold Function. The traditional threshold function is a classic denoising method proposed by Donoho et al. [26] in 1994, which is widely used in the field of signal denoising. The hard threshold function and soft threshold function are defined as equations (5) and (6).

(1) Hard threshold function:

$$\widehat{\mathscr{W}}_{i,k} = \begin{cases} \mathscr{W}_{i,k}, & \left|\mathscr{W}_{i,k}\right| \geq \lambda, \\ 0, & \left|\mathscr{W}_{i,k}\right| < \lambda. \end{cases} \tag{5}$$

(2) Soft threshold function:

$$\widehat{\mathscr{W}}_{i,k} = \begin{cases} \text{sgn}\left(\mathscr{W}_{i,k}\right)\left(\left|\mathscr{W}_{i,k}\right| - \lambda\right), & \left|\mathscr{W}_{i,k}\right| \geq \lambda, \\ 0, & \left|\mathscr{W}_{i,k}\right| < \lambda, \end{cases} \tag{6}$$

where $\mathscr{W}_{i,k}$ is the original wavelet coefficient, $\widehat{\mathscr{W}}_{i,k}$ is the wavelet coefficient after threshold processing, λ is the threshold, and sgn$(*)$ is the sign function. The function curves of the traditional threshold function are shown in Figure 3.

Soft and hard threshold functions have been broadly applied in practical research fields, but these two traditional algorithms still have some disadvantages. In the hard threshold algorithm, $\widehat{\mathscr{W}}_{i,k}$ is discontinuous at $|\mathscr{W}_{i,k}| = \lambda$. This discontinuity easily causes the signal to produce

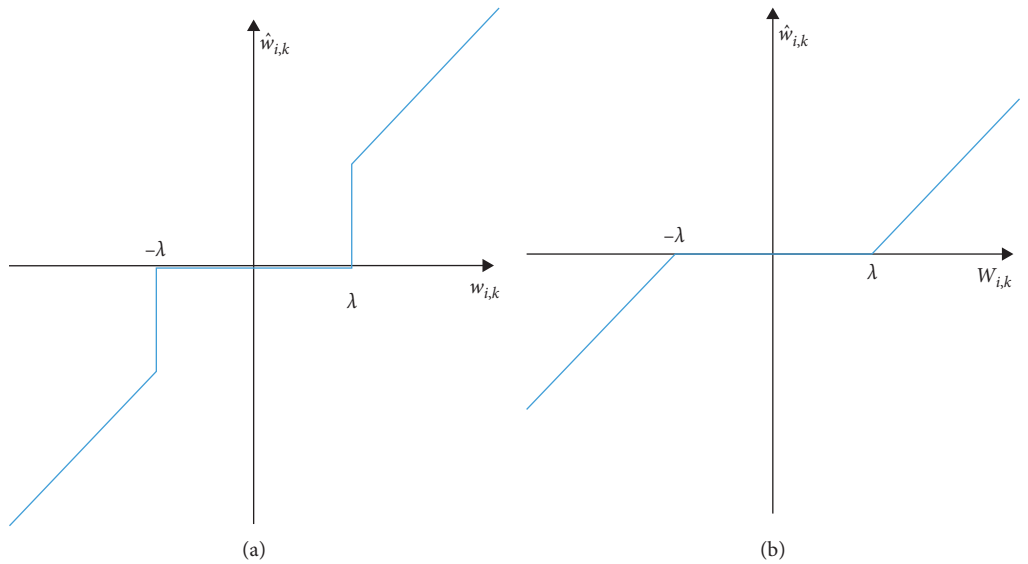

Figure 3: Traditional wavelet threshold function. (a) Hard threshold function. (b) Soft threshold function.

pseudo-Gibbs phenomenon, which makes the reconstructed signal oscillate and not smooth enough. Although the soft threshold function improves the discontinuity of the hard threshold function and ensures the smoothness of the processed signal, the constant deviation between $\widehat{\mathscr{W}}_{i,k}$ and $\mathscr{W}_{i,k}$ may cause distortion of the reconstructed signal, which will directly affect the degree of approximation between the reconstructed signal and the original signal.

3.3.2. Improved Wavelet Threshold Function. For the defects of soft and hard threshold functions, this paper adopts the idea of exponential smoothing approximation, combined with the threshold function construction method in [27], and proposes an improved threshold function. The mathematical expression is given in the following equation:

$$\widehat{\mathscr{W}}_{i,k} = \begin{cases} \operatorname{sgn}\left(\mathscr{W}_{i,k}\right)\left(\left|\mathscr{W}_{i,k}\right| - \dfrac{2\lambda}{1+\exp\left(\alpha\sqrt{\mathscr{W}_{i,k}^2 - \lambda^2}\right)}\right), & \left|\mathscr{W}_{i,k}\right| \geq \lambda, \\ 0, & \left|\mathscr{W}_{i,k}\right| < \lambda. \end{cases} \tag{7}$$

By analyzing the improved threshold function, the following characteristics can be obtained:

(1) It can be seen from equation (7) that the improved threshold function $\widehat{\mathscr{W}}_{i,k}$ is continuous at $|\mathscr{W}_{i,k}| = \lambda$, which surmounts the shortcomings of the hard threshold function.

(2) When $|\mathscr{W}_{i,k}| \longrightarrow \infty$, $\widehat{\mathscr{W}}_{i,k} \longrightarrow \mathscr{W}_{i,k}$, which overcomes the constant deviation between $\widehat{\mathscr{W}}_{i,k}$ and $\mathscr{W}_{i,k}$ in the soft threshold function.

(3) Parameter α is a regulator. When $\alpha = 0$, equation (7) is equivalent to equation (6), and the improved threshold function is a soft threshold function. When $\alpha \longrightarrow \infty$, equation (7) is equivalent to equation (5), and the improved threshold function is a hard threshold function.

To more clearly observe the influence of the value of α on the improved threshold function $\widehat{\mathscr{W}}_{i,k}$, this paper particularly selects $\lambda = 2$ and then draws the improved threshold function curves corresponding to different values of α, as shown in Figure 4.

It can be seen from Figure 4 that when $\alpha = 0$, the improved threshold function is equal to the soft threshold function. When $\alpha = 3$, the improved threshold function is basically equal to the hard threshold function. The improved threshold function can be flexibly adjusted between the hard threshold function and the soft threshold function. It not only combines the preponderances of hard and soft threshold functions but also can flexibly select the corresponding threshold function by adjusting the value of α in the interval [0, 5] ($\alpha > 5$, the denoising effect is basically the same as the hard threshold function), so as to obtain a better resolution than the traditional threshold function.

4. Fast Spectral Correlation

The spectral correlation (SC) can be expressed as

$$S_x(\alpha, f) = E\left\{X\left(f - \frac{\alpha}{2}\right)X^*\left(f + \frac{\alpha}{2}\right)\right\}, \tag{8}$$

where $X(f)$ is the Fourier transform of the signal $x(t)$, $X^*(f)$ is the conjugate of $X(f)$, and α is the cyclic frequency.

The application of SC is limited due to its expensive computing cost. Antoni et al. [20] put forward a fast estimator of the SC using STFT. The principle is to perform Fourier transform on the coefficients of STFT and then return a correlation quantity of the spectral correlation characteristics scanned along the cycle frequency axis. The definition of Fast-SC is as follows:

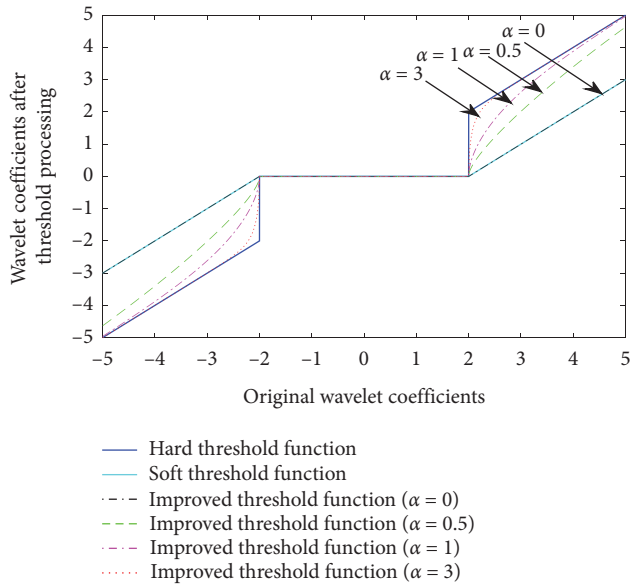

Figure 4: Improved threshold function curves under different values of α.

$$S_x^{\text{Fast}}(\alpha, f) = \frac{\sum_{p=0}^{P} S_x(\alpha, f; p)}{\sum_{p=0}^{P} R_w(\alpha - p\Delta f)} R_w(0), \tag{9}$$

where $S_x(\alpha, f; p)$ is the Fourier transform of the interactions among the STFT coefficients; α is the cyclic frequency; f is the carrier frequency; Δf is the carrier frequency resolution; p is the integer that remains closest to α; R_w is the squared window spectrum.

The formula for spectral coherence is

$$\gamma_x(\alpha, f) = \frac{S_x(\alpha, f)}{\sqrt{S_x(f) S_x(f - \alpha)}}. \tag{10}$$

The exploitation of the Fast-SC realizes a simple and practical implementation to reveal the cyclostationary features in the condition monitoring signals.

5. Simulation Analysis

To study the feasibility of this method, a simulation study was performed to reveal the analysis results at a high noise level. It is assumed that the simulated signal can be expressed as follows [22]:

$$x(t) = \left[\sum_{i=0}^{M-1} D(t - iT)\right] \times \left[A e^{-\xi 2\pi f_n t} \sin\left(2\pi f_n \sqrt{1 - \xi^2}\, t\right)\right] + n(t), \tag{11}$$

where M is the number of fault impulses; D represents the single pulse intensity; T is the time interval between two adjoining impulses; A represents the amplitude of fault impulses; f_n is the inherent frequency and ξ is the damping coefficient. The parameters of outer race fault model are listed in Table 1. In addition, $n(t)$ is random white noise. The sampling frequency is 204,800 Hz, the number of sampling points is 102,400, the SNR is equal to −20 dB, and the fault characteristic frequency is 100 Hz. Figure 5 displays the waveform and spectrum of the simulated signal. It is difficult to identify the fault of bearing from the spectrum, so further analysis is essential.

Table 1: Parameters of the outer race fault model.

M	D	$T(s)$	A	ξ	f_n(Hz)
30	1	1/100	3	0.1	3000

In order to accurately obtain the fault characteristic frequency of the bearing, this method is used to dispose the simulated signal. Firstly, the simulated signal is denoised by improved wavelet threshold denoising algorithm, and then Fast-SC is performed on the denoised signal to detect the fault characteristic frequency of the bearing. Figure 6 shows the spectrum obtained by this method, which can effectively identify the outer race fault characteristic frequency f_o and its harmonics ($2f_o$, $3f_o$, $4f_o$).

To prove the superiority of this method, the simulated signal is dealt with Fast-SC, the combined method based on traditional wavelet threshold and Fast-SC. The comparison results acquired by the above three methods are shown in Figures 7 to 8. Figure 7 displays the spectrum obtained by directly performing Fast-SC on the simulated signal $x(t)$. From Figure 7, although f_o can be identified, its harmonics ($2f_o$, $3f_o$, $4f_o$) cannot be identified due to the interference of numerous noises. Figures 8(a) and 8(b), respectively, show the analysis results of the soft threshold and the hard threshold combined with Fast-SC. From Figures 8(a) and 8(b), only f_o and its harmonic ($2f_o$) can be detected. Its harmonics ($3f_o$, $4f_o$) are overwhelmed by background noise. According to the comparison results, it is observed that the combined method using improved wavelet threshold denoising and Fast-SC is better than Fast-SC and the combined method using traditional wavelet threshold and Fast-SC.

6. Experiment Validation

To determine the reliability of the proposed method, it was further validated using the experimental platform shown in Figure 9. The bearing test bench consists of an electric motor, a coupling, an intermediate shaft, a support bearing, and an electric brake. The measured signals were obtained through a vibration sensor mounted vertically on the bearing housing of the motor drive end with a sensitivity of 1.04mV/ms^2. In this experiment, one vibration sensor is fixed on the rolling bearing seat of the motor drive end, and the other vibration sensor is placed on the supporting rolling bearing seat. The experimental bearing is shown in Figure 10. Its failure mode is the weak fault of the outer race of the motor bearing. Data were sampled at 20 kHz. The kinematical parameters of the experiment bearing are listed in Table 2. According to equation (12), the theoretical outer race fault characteristic frequency of rolling bearing is calculated as 89.33 Hz.

$$f_o = \frac{Z}{2} f_a \left(1 - \frac{d}{D} \cos\alpha\right), \tag{12}$$

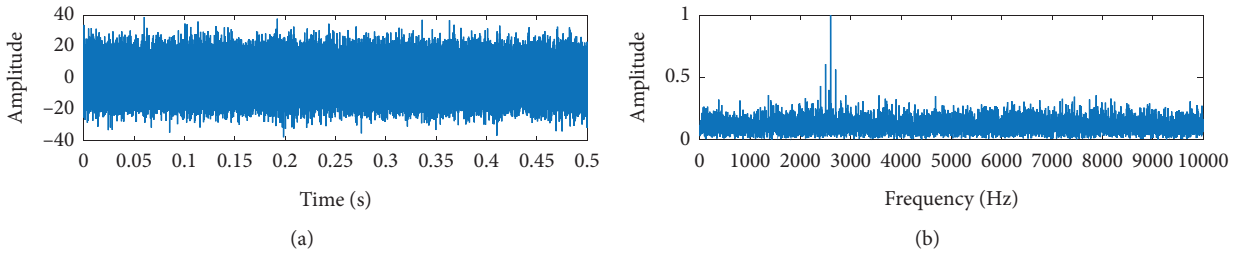

Figure 5: Simulation signal of rolling bearing. (a) Waveform. (b) Spectrum.

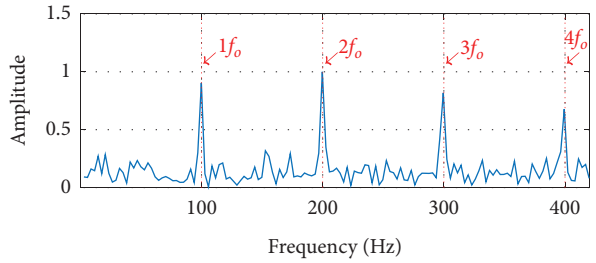

Figure 6: Results of the proposed method.

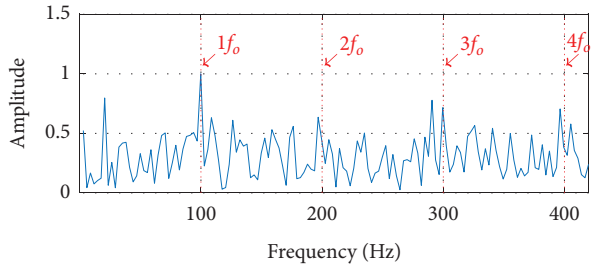

Figure 7: Results of Fast-SC.

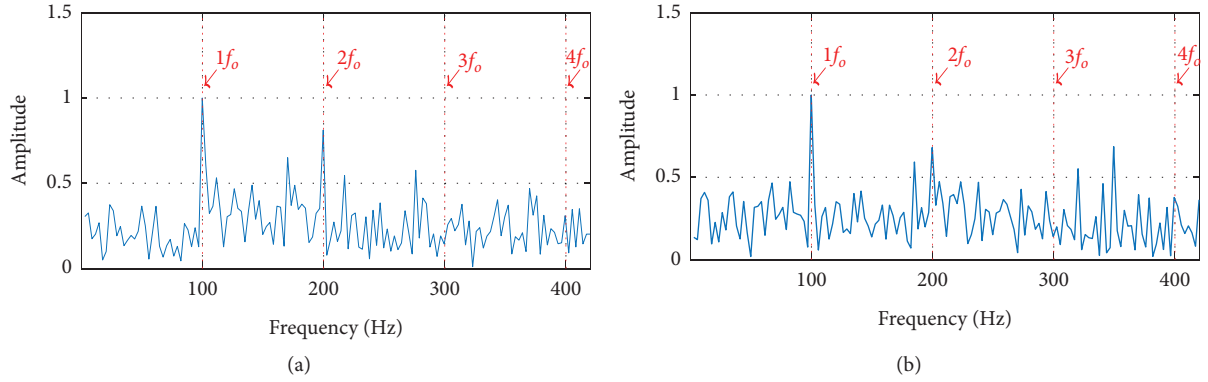

Figure 8: Results of the combined method using traditional wavelet threshold and Fast-SC. (a) Soft wavelet threshold and Fast-SC. (b) Hard wavelet threshold and Fast-SC.

where D is pitch diameter, d is roller diameter, Z is number of rollers, α is contact angle, and $f_a = 24.48$ is shaft rotational frequency.

Figure 11 displays the waveform of the measured signal and its spectrum. It serves to show from Figures 11(a) and 11(b) that the fault characteristic frequency f_o is submerged by strong noise. Similar to simulation analysis, four methods are performed to deal with the measured signal. Firstly, the measured signal is directly processed by Fast-SC, and the result is shown in Figure 12. According to Figure 12, f_o can

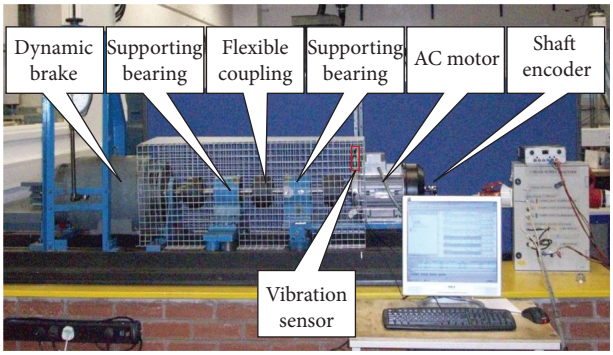

Figure 9: Rolling element bearing test platform.

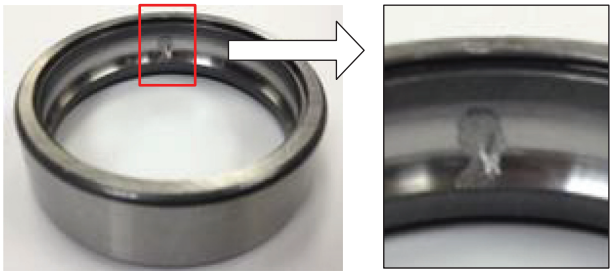

Figure 10: The fault mode: outer race fault.

Table 2: Kinematical parameters of the experimental bearings.

Bearing model	Ball diameter d (mm)	Pitch diameter D_m (mm)	Ball number	Contact angle β
6206ZZ	9.53	46.4	9	0°

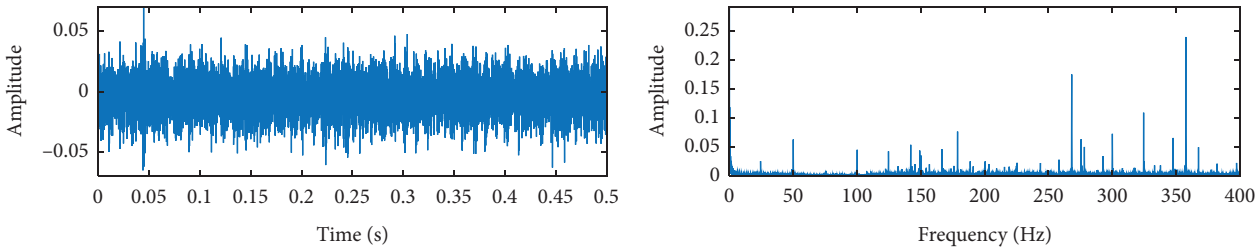

Figure 11: Vibration signal of experimental bearing. (a) Waveform. (b) Spectrum.

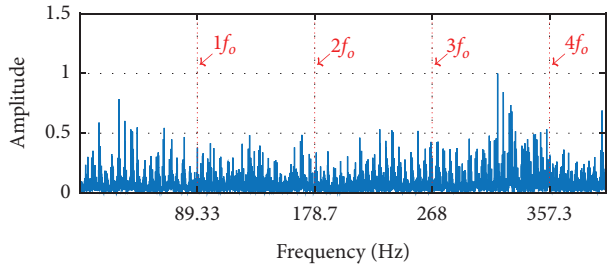

Figure 12: Results of Fast-SC.

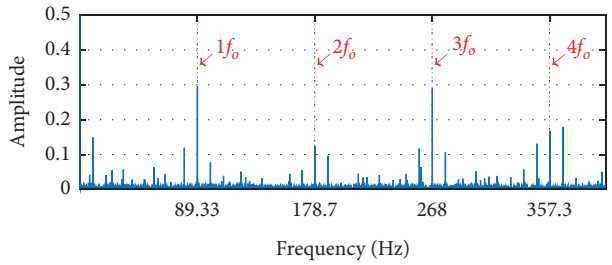

Figure 13: Results of the proposed method.

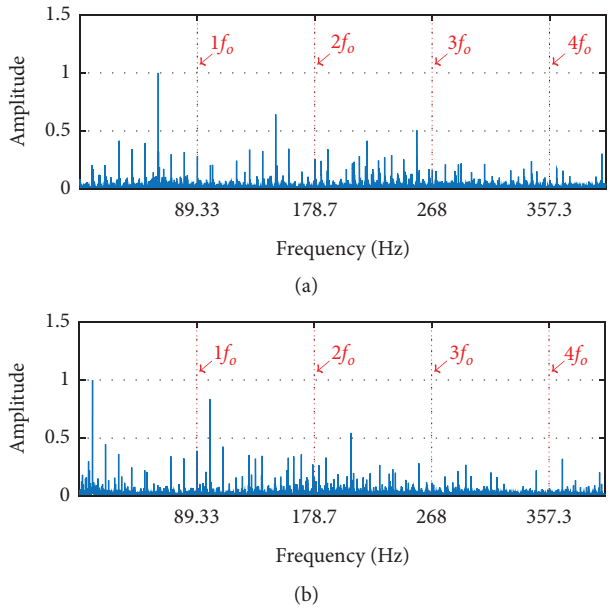

Figure 14: Results of the combined method using traditional wavelet threshold and Fast-SC. (a) Soft wavelet threshold and Fast-SC. (b) Hard wavelet threshold and Fast-SC.

only be identified reluctantly, but its harmonics ($2f_o$, $3f_o$, $4f_o$) are submerged by noise. Next, this approach is employed to process the measured signal. The improved wavelet threshold denoising is firstly adopted to remove the noise component of the measured signal, and then Fast-SC is performed on the denoised signal to extract the related characteristic frequency of the outer race fault of the bearing. The result is displayed in Figure 13, it is observed from Figure 13 that there are distinct peaks at f_o and its harmonics ($2f_o$, $3f_o$, $4f_o$), and it can be concluded that the bearing outer race is damaged.

To reflect the superiority of this method, the effects of the combined method based on soft and hard thresholds with Fast-SC are compared with it. Firstly, the soft and hard wavelet thresholds are, respectively, used to denoise the measured signal, and then the denoised signal is analyzed by using Fast-SC. Figure 14 shows the analysis results, and it can only be seen from Figure 14 that f_o and its harmonic ($2f_o$) have obvious peaks. Compared with Figure 12, there is no significant improvement, and the effect is not as good as that of Figure 13. The above results prove that this method can more effectively extract the fault features of bearings compared with Fast-SC and the combined method using traditional wavelet threshold and Fast-SC.

7. Conclusions

Aiming at the problem that the early fault features of rolling bearings are difficult to be extracted, a fault diagnosis method using the improved wavelet threshold denoising and Fast-SC is proposed. First, the improved wavelet threshold denoising is performed to denoise the original signal to improve its SNR. Then, the denoised signal is analyzed by Fast-SC to detect the fault characteristics of the bearing. Through the simulation analysis and experimental verification, the conclusions are as follows:

(1) The improved wavelet threshold denoising can effectively improve the weakness of Fast-SC which is susceptible to strong background noise when processing nonstationary signals and further highlight the modulation component of the vibration signal.

(2) Fast-SC is used for residual noise suppression and modulation component demodulation of the

denoised signal, which can enhance the periodic components in the signal and improve the accuracy of fault feature extraction.

(3) The validity of this approach is proved by simulation analysis and experimental data. The comparison results show that the analysis effect of the proposed method is better than Fast-SC and the combined method based on traditional wavelet threshold and Fast-SC, and it can more effectively improve the accuracy of rolling bearing fault diagnosis.

(4) Although this method can clearly detect the outer race fault of rolling bearings, there are still interference components. Therefore, how to precisely identify the fault of rolling bearings under strong background noise is the direction of future work. In addition, whether the proposed method can solve other problems, such as gear faults, is also one of the future works.

Data Availability

The datasets supporting the conclusions of this article are included within the article.

Conflicts of Interest

The authors declare that they have no conflicts of interest.

Acknowledgments

This work was supported by the Funds for Creative Research Groups of Hebei Province (no. E2020202142) (reliability of electrical equipment) and the National Natural Science Foundation of China (nos. 51875166 and U1813222).

References

[1] B. Chen, B. Shen, F. Chen et al., "Fault diagnosis method based on integration of RSSD and wavelet transform to rolling bearing," *Measurement*, vol. 131, pp. 400–411, 2019.

[2] W. Huang, H. Sun, J. Luo, and W. Wang, "Periodic feature oriented adapted dictionary free OMP for rolling element bearing incipient fault diagnosis," *Mechanical Systems and Signal Processing*, vol. 126, pp. 137–160, 2019.

[3] D. MaY. X. Lu et al., "Bearing fault diagnosis based on collaborative representation using projection dictionary pair," *Shock and Vibration*, vol. 2019, Article ID 3871089, 13 pages, 2019.

[4] J. Li, J. Zhang, and Y. Zhang, "A novel adaptive stochastic resonance method based on coupled bistable systems and its application in rolling bearing fault diagnosis," *Mechanical Systems and Signal Processing*, vol. 114, pp. 128–145, 2019.

[5] M. Zhao, X. Jia, Y. Lei, and J. Lee, "Instantaneous speed jitter detection via encoder signal and its application for the diagnosis of planetary gearbox," *Mechanical Systems and Signal Processing*, vol. 98, pp. 16–31, 2018.

[6] A. Glowacz, "Fault diagnosis of electric impact drills using thermal imaging," *Measurement*, vol. 171, Article ID 108815, 2021.

[7] Q. He, E. Wu, and Y. Pan, "Multi-scale stochastic resonance spectrogram for fault diagnosis of rolling element bearings," *Journal of Sound and Vibration*, vol. 420, pp. 174–184, 2018.

[8] D. Zhang and D. Yu, "Multi-fault diagnosis of gearbox based on resonance-based signal sparse decomposition and comb filter," *Measurement*, vol. 103, pp. 361–369, 2017.

[9] J. Guo, D. Zhen, H. Li, Z. Shi, F. Gu, and A. D. Ball, "Fault feature extraction for rolling element bearing diagnosis based on a multi-stage noise reduction method," *Measurement*, vol. 139, pp. 226–235, 2019.

[10] F. Cong, J. Chen, G. Dong, and F. Zhao, "Short-time matrix series based singular value decomposition for rolling bearing fault diagnosis," *Mechanical Systems and Signal Processing*, vol. 34, no. 1-2, pp. 218–230, 2013.

[11] K. V. Rajiv and Q. Peng, "Crack detection in the rotor ball bearing system using switching control strategy and Short Time Fourier Transform," *Journal of Sound and Vibration*, vol. 432, pp. 502–529, 2018.

[12] M. Y. Asr, M. M. Ettefagh, and S. N. Razavi, "Diagnosis of combined faults in rotary machinery by non-naive Bayesian approach," *Mechanical Systems and Signal Processing*, vol. 85, pp. 56–70, 2017.

[13] Y. Li, K. Ding, G. He, and X. Jiao, "Non-stationary vibration feature extraction method based on sparse decomposition and order tracking for gearbox fault diagnosis," *Measurement*, vol. 124, pp. 453–469, 2018.

[14] J. Li, M. Li, and J. Zhang, "Rolling bearing fault diagnosis based on time-delayed feedback monostable stochastic resonance and adaptive minimum entropy deconvolution," *Journal of Sound and Vibration*, vol. 401, pp. 139–151, 2017.

[15] H. Li, T. Liu, X. Wu, and Q. Chen, "Research on bearing fault feature extraction based on singular value decomposition and optimized frequency band entropy," *Mechanical Systems and Signal Processing*, vol. 118, pp. 477–502, 2019.

[16] D. Wang, X. Zhao, L.-L. Kou, Y. Qin, Y. Zhao, and K.-L. Tsui, "A simple and fast guideline for generating enhanced/squared envelope spectra from spectral coherence for bearing fault diagnosis," *Mechanical Systems and Signal Processing*, vol. 122, pp. 754–768, 2019.

[17] Z. Y. Chen, A. Mauricio, W. H. Li et al., "A deep learning method for bearing fault diagnosis based on cyclic spectral coherence and convolutional neural networks," *Mechanical Systems and Signal Processing*, vol. 140, Article ID 106683, 2020.

[18] S. Schmidt, P. S. Heyns, and K. C. Gryllias, "A methodology using the spectral coherence and healthy historical data to perform gearbox fault diagnosis under varying operating conditions," *Applied Acoustics*, vol. 158, Article ID 107038, 2020.

[19] C. Y. Liu and K. Gryllias, "A semi-supervised support vector data description-based fault detection method for rolling element bearings based on cyclic spectral analysis," *Mechanical Systems and Signal Processing*, vol. 140, Article ID 106682, 2020.

[20] P. Liu, H. Sohn, and I. Jeon, "Nonlinear spectral correlation for fatigue crack detection under noisy environments," *Journal of Sound and Vibration*, vol. 400, pp. 305–316, 2017.

[21] J. Antoni, G. Xin, and N. Hamzaoui, "Fast computation of the spectral correlation," *Mechanical Systems and Signal Processing*, vol. 92, pp. 248–277, 2017.

[22] J. Li, Q. Yu, X. Wang, and Y. Zhang, "An enhanced rolling bearing fault detection method combining sparse code shrinkage denoising with fast spectral correlation," *ISA Transactions*, vol. 102, pp. 335–346, 2020.

[23] G. J. Tang and T. Tian, "Compound fault diagnosis of rolling bearing based on singular negentropy difference spectrum and integrated fast spectral correlation," *Entropy*, vol. 22, no. 3, Article ID 367, 2020.

[24] D. L. Donoho and I. M. Johnstone, "Ideal spatial adaptation via wavelet shrinkage," *Biometrika*, vol. 81, no. 12, pp. 425–455, 1994.

[25] X. Xu, M. Luo, Z. Tan, and R. Pei, "Echo signal extraction method of laser radar based on improved singular value decomposition and wavelet threshold denoising," *Infrared Physics & Technology*, vol. 92, pp. 327–335, 2018.

[26] D. L. Donoho, "De-noising by soft-thresholding," *IEEE Transactions on Information Theory*, vol. 41, no. 3, pp. 613–627, 1995.

[27] B. Liu, J. L. Feng, S. P. Song et al., "Research on an improved wavelet denoising algorithm with parameter self-tuning," *Control Engineering of China*, vol. 27, no. 3, pp. 444–450, 2020.